Semicond. Sci. Technol. **23** (2008) 045015 (8pp) doi:10.1088/0268-1242/23/4/045015

Absorption and transport properties of Si rich oxide layers annealed at various temperatures

D Nesheva[1], N Nedev[1,2], Z Levi[1], R Brüggemann[3], E Manolov[1], K Kirilov[4] and S Meier[3]

[1] Institute of Solid State Physics, Bulgarian Academy of Sciences, 72 Tzarigradsko Chaussee Blvd, 1784 Sofia, Bulgaria
[2] Instituto de Ingenieria, Universidad Autónoma de Baja California, Benito Juárez Blvd, s/n, C P 21280, Mexicali, Baja California, Mexico
[3] Institute of Physics, Carl von Ossietzky University Oldenburg, D-26111 Oldenburg, Germany
[4] Department of Solid State Physics and Microelectronics, Sofia University 'St Kliment Ohridski', 5 James Bourchier, 1164 Sofia, Bulgaria

E-mail: nesheva@issp.bas.bg

Received 9 November 2007, in final form 31 January 2008
Published 20 March 2008
Online at stacks.iop.org/SST/23/045015

Abstract
Thin films of SiO_x ($x = 1.15$, $d = 1$ and 2 μm), deposited by thermal vacuum evaporation of SiO on n- and p-type crystalline Si or quartz substrates, and then furnace annealed at 250, 700 and 1000 °C, are studied. Optical and infrared transmission measurements prove phase separation upon annealing at 700 and 1000 °C and growth of amorphous Si nanoparticles upon annealing at 700 °C, whose optical band gap is ∼2.6 eV. High-resolution electron microscopy data confirm growth of Si nanocrystals with average size ∼5 nm in the films annealed at 1000 °C. Both kinds of transmission data were used to estimate the nanoparticle volume fraction and values of 0.2–0.25 and 0.25–0.30 for the films annealed at 700 and 1000 °C, respectively, are determined. Current–voltage characteristics (at fields $>5 \times 10^4$ V cm^{-1}) are measured on metal/SiO_x/c-Si/metal structures to explore carrier transport mechanisms in all kinds of samples. They are nearly symmetric, which indicates that in all samples carrier transport via structures is dominated by the transport in the SiO_x layers. It is concluded that current transport is space-charge-limited for the layers annealed at 250 °C. In the films further annealed at 700 °C containing amorphous nanoparticles, Poole–Frenkel transport mechanism is reported while tunnelling is assumed for the films annealed at 1000 °C.

1. Introduction

The prospect for using nanosized silicon as a light source in optoelectronic devices is very attractive since such a source would be compatible with the existing manufacturing infrastructure for silicon integrated circuits [1]. Recently, a number of other interesting effects have also been discovered in Si nanocrystals, such as photoconductive effects [2], resonant tunnelling [3] and memory effect [4, 5]. The potential applications of layers containing nanosized silicon (Si nanocrystals (NCs), amorphous nanoparticles (a-NPs) or both kinds of nanoparticles [6]) require good knowledge of the Si volume fraction, electronic properties of the nanoparticles and carrier transport in the layers.

A variety of transport mechanisms, such as ballistic transport [7], Fowler–Nordheim tunneling [8], Schottky [9] and Poole–Frenkel [10, 11] emission, Coulomb blockade [12, 13] and percolation [14], have been suggested in films containing silicon NCs. Each of these mechanisms is important for practical applications and attracts a great deal of interest. The observation of different transport mechanisms can be understood if one takes into account that the investigated nanostructured materials were fabricated with various structures, nanocrystal volume fractions, surface passivation, etc. If one compares the very large number of

already available data on Si NCs with those for amorphous nanoparticles, it is seen that the latter are still relatively unexplored. There are not many data on their size and electronic properties. On the other hand, amorphous clusters may represent an alternative to NCs because of the lower energy consumption necessary for their fabrication [15–18].

In this paper SiO_x films with initial $x = 1.15$, prepared by thermal evaporation of SiO in vacuum on n- and p-type crystalline Si substrates, are studied. Furnace annealing of some films was carried out to grow amorphous or crystalline silicon nanoparticles. Optical and infrared transmission spectroscopy are applied to estimate the optical band gap of amorphous nanoparticles and the Si volume fraction, which are important quantities for practical applications. Investigations of the electrical transport are also carried out on films containing amorphous or crystalline silicon nanoparticles, as well as on homogeneous SiO_x thin films of the same composition. The I–V curves measured on homogeneous SiO_x layers are mediated by space-charge-limited current (SCLC) transport, while for the films containing amorphous and crystalline nanoparticles, Poole–Frenkel and Fowler–Nordheim tunnelling transport mechanisms, respectively, are suggested.

2. Experimental details

SiO_x layers with a thickness of 1 or 2 μm were prepared by thermal evaporation of SiO at a vacuum of 1×10^{-3} Pa and a deposition rate of 6 nm s^{-1}. Substrates of p- or n-type c-Si (4–6 Ω cm) and fused quartz were used, maintained at room temperature. The composition of these films, determined by means of RBS using 2.4 MeV He ions with a collection of scattered ions at 165° with respect to the incidence direction [19], is $x = 1.15$. The layer with $x = 1.7$ whose transmission spectrum is shown in figure 2 was produced at the same vacuum and a deposition rate of 0.2 nm s^{-1}. More details about the deposition conditions and the effect of the deposition rate and the residual pressure on the film composition can be found in [19]. Before the SiO_x layer deposition, the substrates were cleaned chemically; for the silicon wafers a standard procedure for the microelectronics industry was applied. All deposited films were annealed at 250 °C for 30 min in argon to keep them stable in standard room conditions. Further annealing was carried out in an argon atmosphere for 60 min at 700 °C or in a nitrogen atmosphere at 1000 °C to form amorphous or crystalline nanoparticles, respectively [16, 19]. For the electrical investigations aluminium gate and back contacts were deposited by thermal vacuum evaporation, thus forming Al/c-Si/insulator(SiO_x)/Al (MIS) structures having active area of the devices of 2×10^{-3} cm^2.

Previous Raman scattering measurements performed did not find [19] existence of pure Si phase neither in as-deposited nor in films annealed at 250 °C. The result indicates that unlike the films deposited by most other techniques [20] which contain nanoparticles in the as-deposited state, these films obey the random-network-bonding model. Moreover, no phase separation takes place upon annealing at 250 °C. One can expect that the film homogeneity ensures a better control of the nanoparticle size and a narrower size distribution than in the films containing nanoparticles in the as-deposited state.

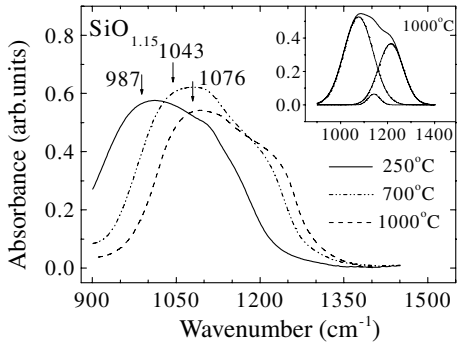

Figure 1. Infrared absorbance spectra of three $SiO_{1.15}$ layers annealed at three different temperatures, denoted in the figure. The inset shows deconvolution of the IR spectrum of the layer annealed at 1000 °C.

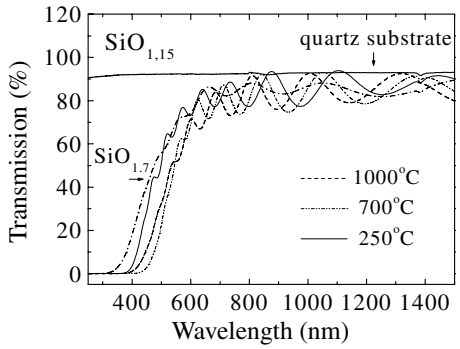

Figure 2. Optical transmission spectra of three $SiO_{1.15}$ layers annealed at three different temperatures, denoted in the figure. Also, optical transmission spectrum of a homogeneous $SiO_{1.7}$ layer ($T_{SiO_{1.7}}$) is depicted.

Optical and infrared (IR) transmission measurements were carried out by Cary 5E and Bruker Vertex 70 spectrophotometers, respectively. The current–voltage (I–V) characteristics were performed by a Keithley 610C electrometer. Since at lower voltages a current increase with time was observed, related in [18] to hole trapping in the SiO_x layer, the current values in the I–V curves at voltages <30 V were measured after achieving quasi-stationary conditions. The polarity of the applied voltage given in the figures below concerns the c-Si substrate (+ means forward bias for the p-Si substrates and reverse bias for the n-Si ones). All measurements were carried out at room temperature.

3. Results and discussion

3.1. Transmission measurements

Figures 1 and 2 show IR absorbance spectra and optical transmission (OT) spectra, respectively, of three SiO_x layers annealed at three different temperatures. A 'blue' shift (to higher frequencies) of the IR absorbance spectra of the films annealed at 700 °C and 1000 °C is observed in figure 1 being

Table 1. Positions of the TO mode in the IR transmission spectra of SiO_x films annealed at different temperatures and the corresponding film or matrix composition and Si nanoparticle volume fraction. The optical band gap and average diameter of the amorphous Si nanoparticles are also given and compared with data of other authors.

Annealing temperature (°C)	Position of the main TO mode (cm^{-1})	SiO_x composition x	E_g^o of Si nanoparticles (eV)	Average nanoparticle diameter (nm)	Volume fraction of nanosized Si
250 no phase separation	987	1.15	–	–	–
700 a-NPs	1043	1.7	2.64 ∼2.4 [26] 2.5 [27]	2.1 2.0 ± 0.8 [6]	0.22 (OT) 0.2 (IR)
1000 NCs	1076	2.0	–	∼5 [33, 34]	0.30 (HREM) 0.30 (OT) 0.26 (IR) 0.27 [38]

stronger upon annealing at 1000 °C. Moreover, an annealing induced 'red' shift (to longer wavelengths) of the optical transmission spectra of the films annealed at 700 and 1000 °C is seen in figure 2.

It is well known [21–23] that the main band in the IR spectra of SiO_2 observed at ∼1080 cm^{-1} is due to an asymmetric stretching vibration of the Si–O–Si bridge. It consists of several modes, a transverse-optical (TO) at 1080 cm^{-1} and others (more than one) longitudinal-optical (LO) in the range 1200–1300 cm^{-1}. The position of the band is shifted to low frequencies ('red' shift) with respect to silica when the oxygen content decreases [23]. Hence, the 'blue' shift of the IR spectra observed upon annealing indicates that phase separation, i.e. formation of pure silicon phase and an increase of the oxygen content in the matrix, takes place upon annealing at both temperatures. Below the IR results are used to make an estimation of the volume fraction of the separated pure silicon phase in the annealed layers. For this purpose, the exact position of the TO mode and the oxygen content of the matrix in the annealed layers had to be determined. Therefore, a deconvolution of the spectra was performed (see the inset in figure 1). Peaks of the fitting functions are situated at 987, 1043 and 1076 cm^{-1} in the films annealed at 250, 700 and 1000 °C, respectively. The position of the main TO mode in the IR transmission spectra of SiO_x films annealed at these temperatures and its relation to the film or the matrix composition are given in table 1 along with the Si nanoparticles volume fraction, optical band gap and average diameter of the amorphous Si nanoparticles determined in sections 3.1 and 3.2. The value of 1043 cm^{-1} corresponds [24] to $x \approx 1.7$ (i.e. the films annealed at 700 °C can be referred to as a nanoparticle–matrix system with Si–$SiO_{1.7}$), while 1076 cm^{-1} corresponds to $x \approx 2$ (Si–SiO_2 films).

The increase of the oxygen content causes an increase of the optical band gap of the SiO_x matrix in the films annealed at high temperatures and one can expect a 'blue' shift of its optical transmission spectra. Instead, a 'red' shift is observed (see figure 2) which should be due to absorption in the pure silicon phase formed. In order to estimate the contribution of the 'pure' Si phase to the total absorption of the Si–$SiO_{1.7}$ layer we subtracted the transmission curve of the layer annealed at 700 °C (T_{700}) from the transmission curve of a homogeneous $SiO_{1.7}$ layer ($T_{SiO_{1.7}}$) with the same thickness

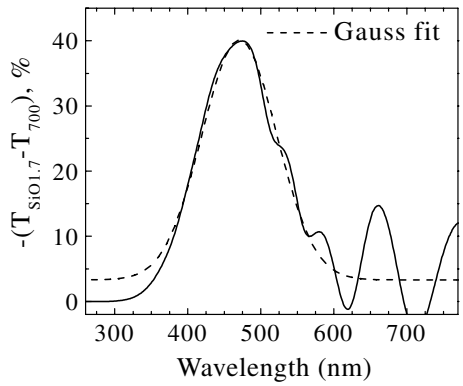

Figure 3. A curve obtained by subtraction of the transmission curve of a $SiO_{1.15}$ layer annealed at 700 °C (T_{700}) from the transmission curve of a $SiO_{1.7}$ ($T_{SiO_{1.7}}$) which represents the absorption of the pure Si phase in the annealed layer. The dashed line is a Gaussian fit.

and composition as that of the matrix. The result is a Gaussian band (see figure 3) peaked at ∼470 nm (2.64 eV). This band represents the optical absorption of the 'pure' silicon phase and its maximum energy can be considered as an average value of the optical band gap (E_g^o) of the amorphous Si particles. It is significantly greater than E_g^o of amorphous silicon thin films (∼1.5 eV [25]), thus indicating the formation of nanosized amorphous Si. A value $E_g^o \approx 2.4$ eV has been determined from the Tauc plot of the absorption spectra of films prepared by pulse-laser deposition at room substrate temperature and annealed for 60 min at 600 °C, which contains amorphous Si nanoparticles [26]. However, it should be noted that those films contain amorphous nanoparticles in as-deposited state (with $E_g^o \approx 2.9$ eV) and one could expect a smaller size in our samples which are homogeneous before the high temperature annealing. Also, a value of ∼2.5 eV has been obtained for the 'Tauc' gap of Si nanoparticles in $SiO_{1.1}$ films deposited by co-sputtering and annealed at 300 °C for 120 min [27]. Again, it is a bit smaller than our value, but these films also showed initial phase separation in the as-deposited state. The approach used here for the determination of E_g^o is not affected by the method of processing the absorption spectrum (Tauc or Cody presentation).

From the curve shown in figure 3 one could also get an idea of the average size and size distribution of

the amorphous nanoparticles provided an experimental or theoretical dependence of E_g^o on the nanoparticle size is available. Since there are no such curves for amorphous Si nanoparticles, we used the experimental dependence of the absorption gap versus Si nanocrystal diameter given in [1] to make a rough estimation of the nanoparticle size. A value of 2.1 nm has been obtained for the average diameter d which is much smaller than the nanocrystal diameter in samples annealed at 1000 °C (see below). The investigations performed in [6] by energy-filtered transmission electron microscopy on SiO_x films with very similar initial composition prepared by plasma enhanced chemical vapour deposition have shown growth of a-Si nanoparticles with $d = 2.0 \pm 0.8$ nm upon annealing at higher temperatures ($T \geqslant 900$ °C). Hence, the value of 2.1 nm we determined seems quite acceptable. Furthermore, based on the Gaussian curve in figure 3 and the mentioned dependence in [1], a value of < 0.4 nm has been drawn for half-width at half-maximum of the nanoparticle size distribution, η. Thus, for the η/d ratio in the films containing amorphous Si particles one obtains <19% for the particle size distribution. It is very similar to the size distribution of Si NCs in samples with $x = 1.17$, prepared by thermal evaporation of SiO and annealed at 1000 °C for 60 min [28]. To our knowledge this is the first estimation of the size distribution of amorphous Si nanoparticles.

3.2. Determination of the silicon volume fraction

Composite materials are systems of conducting or semiconducting nanoparticles (filler) embedded in a dielectric matrix. When the volume fraction of the filler increases, the distance between the filler particles decreases; at a certain concentration contact between certain adjacent particles occurs and two- or three-dimensional networks of nanocrystalline semiconductor particles are formed. The dc electrical conductivity of the system strongly increases and carrier transport mechanism changes. The formation and nature of such a network depends on the chemical composition, volume fraction, sizes and size distribution of the semiconducting nanocrystals [29]. Monte Carlo simulations of Si NC ripening showed [30] that the 'percolation limit' (i.e. the Si excess concentration above which instead of isolated Si NC, Si agglomerates or wires are formed) lies roughly between 10 vol% and 25 vol% depending on annealing time and temperature. However, significantly higher values of the volume fraction of Si nanocrystals (filling factor f) with $f = 0.33$ [31] and $f = 0.38$ [32] have been experimentally obtained for Si rich SiO_2 films, which have been related to a different amount of structural randomness of the semiconducting nanoclusters inside the matrix material. Therefore, in order to make conclusions about the transport mechanism one should know the filling factor of the system.

The high-resolution electron microscopy (HREM) study we performed on films annealed at 1000 °C has shown [33, 34] formation of silicon nanocrystals having average size of ~5 nm. As seen from figure 4, they are randomly distributed in the oxide matrix and apparently do not form percolation paths. A rough estimation f based on this cross-section

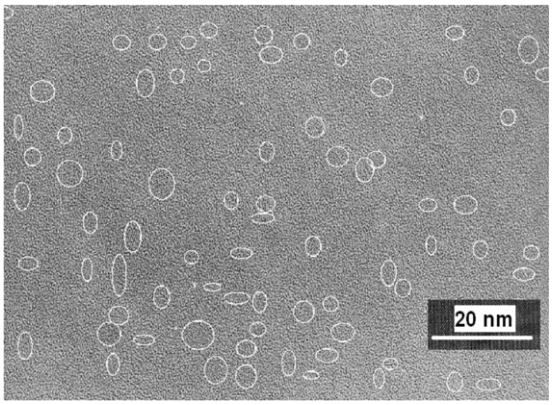

Figure 4. Cross-section TEM micrograph of a-$SiO_{1.15}$ annealed in nitrogen at 1000 °C for 60 min. The circles and ovals represent Si nanocrystals.

micrograph has given $f \approx 0.30$. However the accuracy of such an estimation is rather low since amorphous Si nanoparticles [6] or amorphous shells around a crystalline core could exist but not be seen in the micrograph. On the other hand, some not well-ordered areas could be considered by mistake as nanocrystals. Therefore we used both kinds of transmission measurements to determine f.

The interference seen in figure 2 is due to the difference between the refractive indices of the film and the quartz substrate. In the range of weak absorption the refractive index n and the thickness d of the layers can be calculated applying the approach described in [35]. Values $n_{700} = 2.0$ and $n_{1000} = 1.97$ have been obtained for films annealed at 700 and 1000 °C, respectively as well as $n_{SiO_{1.7}} = 1.65$ for the film with $x = 1.7$ annealed at 250 °C. It has also been confirmed that the layer thickness of all layers studied coincides, in the frame of an experimental error of 5%, with the thickness measured during film deposition. The effective medium approach in the formalism described in [36] gives the following relation between the average dielectric constant ε of a composite medium and the dielectric constants of both constituent materials (written for a Si–SiO_x layer), which is valid for any value of the filling factor f:

$$f = (\varepsilon - \varepsilon_m)(\varepsilon_{Si} + 2\varepsilon_m)/[(\varepsilon_{Si} - \varepsilon_m)(\varepsilon + 2\varepsilon_m) + (\varepsilon - \varepsilon_m)(\varepsilon_{Si} + 2\varepsilon)] \quad (1)$$

where ε_m and ε_{Si} are the dielectric constants of the matrix (SiO_x) and the filler (Si), respectively. In the weak absorption range $\varepsilon \approx n^2$ and applying this relation to equation (1), one can make an estimation of f (without taking into account strain effects). Using $n_{700} = 2.0$, $n_{1000} = 1.97$, $n_{Si} = 3.48$, $n_{SiO_2} = 1.5$ and $n_{SiO_{1.7}} = 1.65$, values $f_{700} = 0.22$ (0.27, when taking into account the observed size-induced decrease of the dielectric constant of Si down to $\varepsilon_{Si} = 9.6$ [37]) and $f_{1000} = 0.30$ (0.35 when $\varepsilon_{Si} = 9.6$) have been obtained for films annealed at 700 and 1000 °C, respectively. The value for $f_{1000} = 0.30$ is close to the filling factor $f_{1000} = 0.27$ obtained in films with similar ($x = 1.1$) initial composition, determined on the basis of Rutherford backscattering data [38] while the assumption for size-induced permittivity reduction gives a much higher f value.

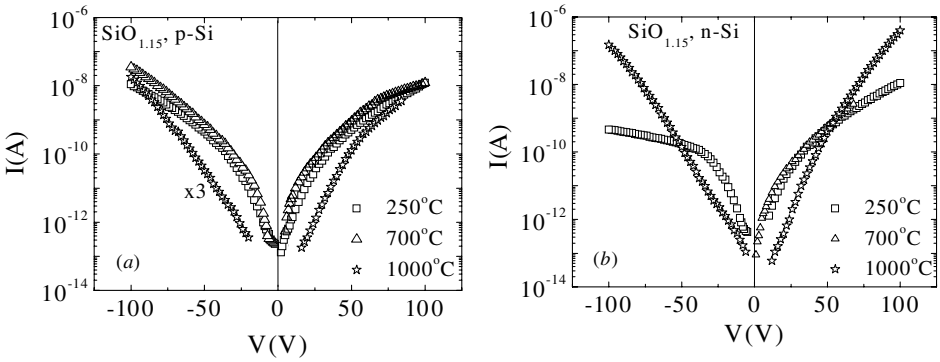

Figure 5. *I–V* characteristics of $SiO_{1.15}$ layers deposited on (*a*) p-Si and (*b*) n-Si annealed at three temperatures denoted in the figures.

An approximate value of the filling factor can also be obtained using the shift of the main TO band in the IR spectra. Assuming that the number of oxygen atoms in the homogeneous layer and the matrix of the annealed films is the same, one can find the following relation between f and the atomic densities of the initial layer ρ_{SiO_x} and pure silicon phase ρ_{Si}:

$$f = (\rho_{SiO_x}/\rho_{Si})(x+1)^{-1}[1-(x/y)] \tag{2}$$

where x is the initial oxygen content and y is the oxygen content in the matrix of the annealed layers. In order to calculate f one can use $\rho_{SiO_x} = 6.6 \times 10^{22}$ cm^{-3} [15], $\rho_{Si} = 5 \times 10^{22}$ cm^{-3}, $x = 1.15$ and $y = 1.7$ or 2.0. Values $f_{700} = 0.2$ and $f_{1000} = 0.26$ are obtained which are in good agreement with the results reported in [15, 38]. We note that values between 5.8×10^{22} cm^{-3} and 6.0×10^{22} cm^{-3} are reported for $x = 1.15$ in [39] which will result in a reduction of the filling factor with ∼10%. As a whole, the silicon volume fractions calculated from the IR data are a bit smaller than those obtained from the optical transmission data and this difference can be understood bearing in mind the uncertainty in the ρ_{SiO_x} and also that the y and $n_{SiO_{1.7}}$ values are not determined very precisely. Thus, the maximum volume fraction of the pure Si phase obtained from the transmission data is $f_{700} = 0.25$ and $f_{1000} = 0.30$ which is less than the experimental threshold values reported by other authors [32, 35] and one can think that no nanoparticle network exists in both kinds of layers. This conclusion is in good agreement with the electron microscopy results (figure 4) as well as with the assumption made in [38] for films with initial oxygen content $x = 1.1$.

3.3. Carrier transport mechanisms

The basic conduction processes in homogeneous insulators, as considered by Sze [40], are: (i) ohmic-like conduction with current density J described as

$$J \propto E \exp[-E_a/kT] \tag{3}$$

(E is the applied field, E_a is the thermal activation energy, k is the Boltzmann constant); (ii) Schottky emission

$$J \propto T^2 \exp\{[-q\Phi_b - (qE/4\pi\varepsilon_i)^{1/2}]/kT\}, \tag{4}$$

that is thermionic emission across the metal–insulator interface or the insulator–semiconductor interface (q equals 1.6×10^{-19} C, Φ_b is the barrier height, ε_i is the insulator dynamic permittivity); (iii) Poole–Frenkel emission,

$$J \propto E \exp\{[-q\Phi_b - (qE/\pi\varepsilon_i)^{1/2}]/kT\}, \tag{5}$$

that is field-enhanced thermal excitation of trapped electrons into the conduction band; (iv) tunnelling,

$$J \propto E^2 \exp[-4(2m^*)^{1/2}(2\Phi_b)^{3/2}/3q\hbar E], \tag{6}$$

which may take place from the metal or semiconductor Fermi level to the insulator conduction band; in the particular case of semiconductor nanoparticles in an insulating matrix, it can occur between nearest nanoparticles; (v) space-charge-limited current (SCLC),

$$J \propto 8\varepsilon_i \mu V^2/9d^3, \tag{7}$$

where d is the distance between the contacts (i.e. the insulator thickness) and μ is the carrier drift mobility. Space-charge-limited currents can take place in insulating materials when carriers are injected and no compensating charge is present.

Figure 5 shows nearly symmetric I–V characteristics of layers deposited on p-Si and n-Si annealed at three different temperatures. It is known that when the transport via MIS structures with a thin isolator film (<100 nm) is controlled by the properties of the insulator–semiconductor or semiconductor–metal interfaces, the I–V characteristics are asymmetric (as an example see [18]). The observed symmetry indicates that current transport through the MIS structures is controlled by the transport in the SiO_x layers. It is seen that the curves of the samples annealed at 250 °C and 700 °C look quite similar while the characteristics of the films annealed at 1000 °C are different. Also, unexpectedly, in most samples the current under reverse bias is a bit higher than that under forward bias. We have not found an explanation of this observation yet.

Figure 6 depicts the I–V characteristics of SiO_x layers having thickness of 1 or 2 μm, which were annealed at 250 °C, now presented in coordinates corresponding to SCLC transport mechanism. It is seen that at applied field $>10^4$ V cm^{-1} the characteristics are linear over more than three orders of magnitude of the current. Also, the scaling law $I/d = F(V/d^2)$ (F means 'function of') proposed by Lampert and Mark [41] is, in some respects, confirmed. These observations allow us to assume that SCLC is the dominant transport

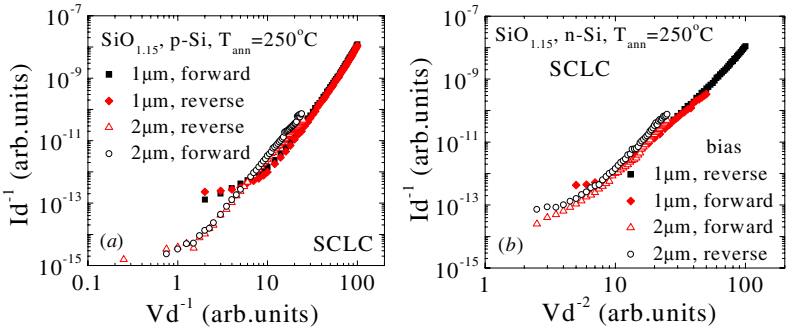

Figure 6. *I–V* characteristics of $SiO_{1.15}$ layers having thickness of 1 or 2 μm annealed at 250 °C presented in coordinates corresponding to SCLC transport mechanism. The layers were deposited on (*a*) p-Si and (*b*) n-Si substrates and the measurements were carried out under forward or reverse bias.

(This figure is in colour only in the electronic version)

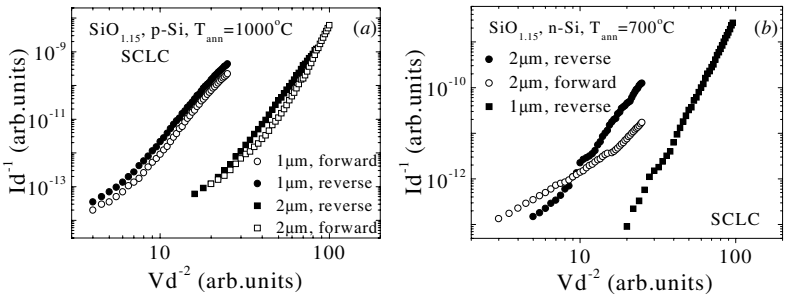

Figure 7. *I–V* characteristics of SiO_x layers having thickness of 1 or 2 μm presented in coordinates corresponding to SCLC transport mechanism. The films were annealed at (*a*) 1000 °C or (*b*) 700 °C. The bias conditions and type of substrates are denoted in the figures.

mechanism in the homogeneous $SiO_{1.15}$ films. It should be noted that the slope of the curves in figure 6 is not 2 as can be expected on the basis of equation (7); it is about 4. As known [41], in disordered materials (such as bulk glasses and amorphous thin films) there exists a high concentration of own defects that most frequently have an exponential distribution. When the quasi-Fermi level moves across such an exponential trap distribution characterized by an energy E_t, the *I–V* characteristic of the MIS structure is described by the formula [41]

$$J \approx q\mu N_c(\varepsilon_i/eN_oE_t)^l\ (V^{l+1}/d^{2l+1}), \qquad (8)$$

where N_c is the conduction band density of states and $l = (E_t/kT) > 2$. If $l = 3$, $\log(J/d) \propto \log[e\mu N_c(\varepsilon/eN_oE_t)^l] + \log(V^4/d^8) = \text{constant} + 4\log(V/d^2)$, which indicates that the slope of the curves should be 4. Based on this consideration a conclusion can be drawn that in the SiO_x layers annealed at 250 °C the SCLC carrier transport is mediated by an exponential trap distribution having $E_t \approx 78$ meV.

In figure 7 the presentation of the *I–V* characteristics of the films annealed at higher temperatures in SCLC coordinates indicates that though in some samples the characteristics look linear, the scaling law is not confirmed which implies a different transport mechanism. Di Maria *et al* [42] were the first to assume that carrier transport in the films containing Si nanoparticles (Si–SiO_2 films) is carried out by direct tunnelling of electrons from one nanocrystal to another. The electrons from the metal contact or the Si substrate reach nearest

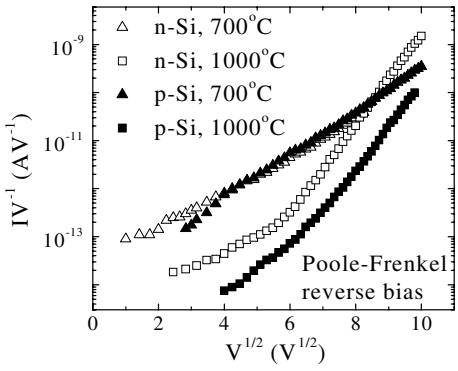

Figure 8. Poole–Frenkel presentation of the *I–V* curves of samples annealed at high temperatures.

to the contact nanocrystals by direct tunnelling, as well. Later many authors claimed observation of electron tunnelling between Si or Ge nanocrystals embedded in oxide matrices ([18, 43] and references therein). Although the current for the tunnelling mechanism should be thermally independent, various temperature dependences have been observed [12, 18, 44, 45] ascribed to different origins such as Poole–Frenkel [18] or Schottky emission [44], the discrete structure of the valence and conduction bands [12] etc.

Figure 8 shows a Poole–Frenkel presentation of the *I–V* curves of samples annealed at 700 and 1000 °C, seen in

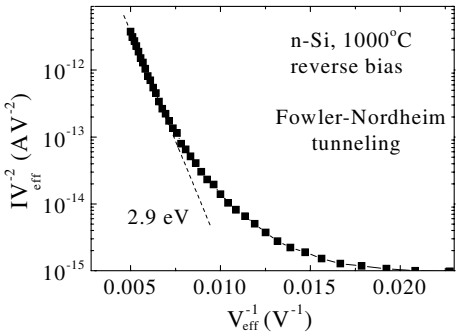

Figure 9. Presentation of the reverse bias *I–V* characteristic of a 1 μm thick SiO_x layer on n-Si substrate annealed at 1000 °C in coordinates corresponding to Fowler–Nordheim tunnelling between Si NCs. The same characteristic is shown in figure 8 in Poole–Frenkel coordinates, as well.

figure 7. The linearity of the curves at high applied voltages indicates that carrier injection in traps and their subsequent emission should be one important transport process in these layers. However, the different slopes seen for samples containing a-Si NP and NCs imply that other processes could also play a role.

Based on the slope A of the curves in figure 8 ($A^{700\,^\circ C} = 1$ and $A^{1000\,^\circ C} = 2.15$), using the relation $A = (q/d\pi\varepsilon_o\varepsilon_{Si-SiO_x})^{1/2}/kT$ [40] one can calculate the dielectric constant of the annealed films. With $T = 300$ K, $kT = 0.026$ eV, $d = 1 \times 10^{-6}$ m, $\varepsilon_o = 8.85 \times 10^{-12}$ F m^{-1}, $q = 1.6 \times 10^{-19}$ C we obtained $\varepsilon^{700\,^\circ C}_{Si-SiO_x} = 8.39$ and $\varepsilon^{1000\,^\circ C}_{Si-SiO_2} = 1.84$.

On the other hand ε_{Si-SiO_x} can be calculated applying the equation [46]

$$\varepsilon_{Si-SiO_x} = \varepsilon_m[1 + (2/3)f\chi]/[1 - (1/3)f\chi], \qquad (9)$$

where $\chi = 3(\varepsilon_{Si} - \varepsilon_m)/(\varepsilon_{Si} + 2\varepsilon_m)$. Using $\chi^{700\,^\circ C} = 0.22$, $\chi^{1000\,^\circ C} = 0.30$, $\varepsilon_{Si} = 11$ and assuming $\varepsilon_m{}^{700\,^\circ C}$ (i.e. $\varepsilon_{x=1.7}$) $= 7$ and $\varepsilon_m{}^{1000\,^\circ C}$ (i.e. $\varepsilon_{x=2.0}$) $= 4$, values $\varepsilon^{700\,^\circ C}_{Si-SiO_x} = 7.77$ and $\varepsilon^{1000\,^\circ C}_{Si-SiO_2} = 5.48$ have been obtained for the samples annealed at 700 °C and 1000 °C, respectively. The two values for the films annealed at 700 °C ($\varepsilon^{700\,^\circ C}_{Si-SiO_x} = 7.77$ and 8.39) differ by less than 10% which confirms the assumption of the Poole–Frenkel transport mechanism. However, the value $\varepsilon^{1000\,^\circ C}_{Si-SiO_2} = 1.84$ is about three times smaller than that obtained from equation (9). It implies that in these samples carrier transport is not mediated by the Poole–Frenkel mechanism and one can assume that for applied voltages $V > 20$ V ($E > 2 \times 10^5$ V cm^{-1}) Fowler–Nordheim tunnelling between the nanocrystals takes place. Based on equation (6) Φ_b can be determined from the slope of the experimental curves in coordinates (I/V^2) versus $(1/V)$ (see figure 9). Keeping in mind the discussion [47] on electric field enhancement we assumed that the average nanoparticle diameter is 5 nm, the average thickness of the barriers between the crystals is also 5 nm and the conductivity of the barriers is much less than that of the nanocrystals (i.e. the effective voltage V_{eff} applied on the barriers is twice as great as the experimental one). A value of $\Phi_b \approx 2.9$ eV has been obtained which is close to that of the barrier for electrons at the Si–SiO_2 interface (~3.1 eV). Based on this result, one can suggest that most likely in the NC-Si–SiO_2 films tunnelling is the dominant carrier transport mechanism.

Electrical transport of dark carriers has already been investigated in Al/Si-rich SiO_2 (1 μm thick)/crystalline p-Si/Al structures [48]. The initial composition of the SiO_x films was $x = 1.5$ and the films were annealed at 1000 °C for 60 min before the deposition of the metal contacts. The nanocrystal Si volume fraction calculated when using equation (2) is ~13%. Space-charge-limited currents have been considered as the main carrier transport mechanism in those films at both forward and reverse applied fields $>10^4$ V cm^{-1}. This result differs from the observations here on the SiO_x films with $x = 1.15$ annealed at both 700 and 1000° C, but it is similar to that obtained for $SiO_{1.15}$ films annealed at 250 °C (in which no phase separation occurs). The difference indicates that perhaps at low filling factor Si NPs do not appreciably affect carrier transport via the Si-rich SiO_x composite layer and one can expect SCLC in the SiO_x matrix. Based on the results of this study one can think that NPs influence the transport at high enough $f > 0.18$. The effect again depends on f; tunnelling can be expected at high volume fractions of pure Si (but still below the percolation threshold) and the Poole–Frenkel mechanism can be observed at intermediate filling factors.

4. Conclusions

Optical and IR transmission as well as electrical transport in SiO_x thin films ($x = 1.15$), deposited by thermal vacuum evaporation of SiO on n- and p-type crystalline Si substrates, and then furnace annealed at 250, 700 and 1000 °C have been investigated. The transmission data have indicated that phase separation takes place upon annealing at 700 and 1000 °C. High-resolution electron microscopy measurements confirmed the growth of Si nanocrystals with an average size of ~5 nm in films annealed at 1000 °C. Moreover, a value of 2.64 eV has been obtained for the optical band gap of amorphous Si nanoparticles grown upon annealing at 700 °C. Using experimental data for the relation of optical band gap versus average diameter of Si NCs, a value of 2.1 nm has been determined for the average diameter of the amorphous NPs. The filling factor has been estimated from the transmission data in the visible and IR spectral range. Values of 0.2–0.25 and 0.25–0.30 have been obtained for the volume fractions of the pure silicon phase in films annealed at 700 and 1000 °C, respectively. They are below the filling factors at which percolation has been observed in Si–SiO_2 layers and therefore it has been concluded that no percolation takes place in the carrier transport via the annealed layers. Nearly symmetric I–V characteristics (at applied fields $>5 \times 10^4$ V cm^{-1}) have been measured on all MIS structures, which show that carrier transport via the structures is dominated by the SiO_x layers. The analysis of the I–V curves in coordinates corresponding to several carrier transport mechanisms has indicated that the current is space-charge-limited in the layers annealed at 250 °C. For the films annealed at 700 °C, containing amorphous nanoparticles, the conclusion of a Poole–Frenkel

transport mechanism is made while for the layers annealed at 1000 °C Fowler–Nordheim tunnelling is suggested. Based on previous and the current results, it is assumed that at low filling factor Si NPs do not appreciably affect carrier transport via the SiO_x matrix of Si-rich SiO_x composite layers. They influence the transport at high enough $f > 0.18$ as tunnelling can be expected at silicon volume fractions close to the percolation threshold while the Poole–Frenkel mechanism is possible at intermediate filling factors.

Acknowledgments

This work has been supported by the Bulgarian Ministry of Education and Science (BMES) under grant NT-4-1 and jointly by BMES and DAAD, Germany under grant D-01-78.

References

[1] Ossicini S, Pavesi L and Priolo F 2003 *Light Emitting Silicon for Microphotonics* (*Springer Tracts in Modern Physics* vol 194) (Berlin: Springer) pp 1–74, chapter 1
[2] Ando M, Miyamoto H, Naito H and Kanemitsu Y 2002 *J. Non-Cryst. Solids* **1084** 299–302
[3] Wan Q, Wang T H, Zhu M and Lin C L 2002 *Appl. Phys. Lett.* **81** 538–40
[4] Tiwari S, Rana F, Hanafi H, Hartstein A, Crabbé E and Chan K 1996 *Appl. Phys. Lett.* **68** 1377–9
[5] De Salvo B, Ghibaudo G, Luthereau P, Baron T, Buffet N, Guillaumot B and Reimbold G 2001 *Solid-State Electron.* **45** 1513–9
[6] Iacona F, Bongiorno C, Spinenella C, Boninelli S and Priolo F 2004 *J. Appl. Phys.* **95** 3723–32
[7] Torchynska T V 2002 *J. Appl. Phys.* **92** 4019–23
[8] Walters R J, Bourianoff G I and Atwater H A 2005 *Nature Mater.* **4** 143–6
[9] Smit G D J, Rogge S and Klapwijk T M 2002 *Appl. Phys. Lett.* **81** 3852–4
[10] Ben-Chorin M, Möller F and Koch F 1994 *Phys. Rev.* B **49** 2981–4
[11] Ioannou-Sougleridis V, Ouisse T, Nassiopoulou A G, Bassani F and Arnaud d'Avitaya F 2001 *J. Appl. Phys.* **89** 610–4
[12] Ciurea M L, Draghici M, Iancu V, Reshotko M and Balberg I 2003 *J. Lumin.* **102–103** 492–7
[13] Pooley D M, Ahmed H, Mizuta H and Nakazato K 2001 *J. Appl. Phys.* **90** 4772–6
[14] Ben-Chorin M, Möller F and Koch F 1995 *Phys. Rev.* B **51** 2199–213
[15] Rinnert H, Vergnat M and Burneau A 2001 *J. Appl. Phys.* **89** 237–43
[16] Nesheva D, Raptis C, Perakis A, Bineva I, Aneva Z, Levi Z, Alexandrova S and Hofmeister H 2002 *J. Appl. Phys.* **92** 4678–83
[17] Rinnert H and Vergnat M 2003 *Physica* E **16** 382–7
[18] Irrera A *et al* 2006 *Nanotechnology* **17** 1428–36
[19] Nesheva D, Bineva I, Levi Z, Aneva Z, Merdzhanova Ts and Pivin J C 2003 *Vacuum* **68** 1–9
[20] Hayashi S and Yamamoto K 1996 *J. Lumin* **70** 352–62
[21] Lehmann A, Schumann L and Hubner K 1984 *Phys. Status Solidi* b **121** 505–11
[22] Shabalov A L and Feldman M S 1987 *Thin Solid Films* **151** 317–23
[23] Tsu D V, Lucovsky G and Davidson B N 1989 *Phys. Rev.* B **40** 1795–805
[24] Bineva I 2004 *PhD Thesis* advisor D Nesheva, Sofia, Bulgaria
[25] Fournier Y and van Dong N 1985 *Phys. Status Solidi* a **88** 309–14
[26] Yoshida K, Umezu I, Sakamoto N, Inada M and Sugimura A 2002 *J. Appl. Phys.* **92** 5936–41
[27] Chen X Y, Lu Y F, Wu Y H, Cho B J, Song W D and Day D Y 2004 *J. Appl. Phys.* **96** 3180–6
[28] Kahler U and Hofmeister H 2002 *Appl. Phys.* A **74** 13–7
[29] Bera S K, Chaudhurl S and Pal A K 2000 *J. Phys. D: Appl. Phys.* **33** 2320–6
[30] Müller T, Heinig K-H and Möller W 2002 *Appl. Phys. Lett.* **81** 3049–2
[31] Shimakawa K 2001 *Proc. 11th ISCMP Materials for Information Technology in the New Millenium* ed J M Marshall, A G Petrov, A Vavrek, D Nesheva, D Dimova-Malinovska and J M Maud (Bath: Bookcraft) pp 1–12
[32] Balberg I 2002 *Proc. Int. Semiconductor Conf. CAS 2002 (Sinaia, Romania)* (Piscataway, NJ: IEEE) vol 1 pp 99–102
[33] Nedev N, Nesheva D, Manolov E, Brüggemann R, Meier S, Kirilov K and Levi Z 2007 *J. Optoelectron. Adv. Mater.* **9** 182–5
[34] Nesheva D, Nedev N, Manolov E, Bineva I and Hofmeister H 2007 *J. Phys. Chem. Solids* **68** 725–8
[35] Swanepoel R 1983 *J. Phys. E: Sci. Instrum.* **16** 1214–22
[36] Granqvist C G and Hundery O 1977 *Phys. Rev.* B **16** 3513–34
[37] Ding L, Chen T P, Liu Y, Liu Y C and Fung S 2005 *Appl. Phys. Lett.* **87** 121903–3
[38] Gallas B, Stenger I, Kao C-C, Fisson S, Vuye G and Rivory J 2005 *Phys. Rev.* B **72** 155319–10
[39] van Hapert J J, Vredenberg A M, van Faassen E E, Tomozeiu N, Arnoldbik M and Habraken F H P M 2004 *Phys. Rev.* B **69** 245202–8
[40] Sze S M 1969 *Physics of Semiconductor Devices* (New York: Wiley) p 496
[41] Lampert M A and Mark P 1970 *Current Injection in Solids* (New York: Academic)
[42] Di Maria D J, Kirtley J R, Pakulis E J, Dong D W, Kuan T S, Pesavento F L, Theis T N, Cutro J A and Brorson S D 1984 *J. Appl. Phys.* **56** 401–16
[43] Nesheva D 2006 *Handbook of Semiconductor Nanostructures and Devices* vol 1, ed A A Balandin and K L Wang (Stevenson Ranch, CA: American Scientific Publishers) pp 453–97 chapter 10
[44] Lombardo S and Campisano S U 1996 *Mater. Sci. Eng.* **R17** 281–332
[45] Burr T A, Seraphin A A, Werwa E and Kolenbrander K D 1997 *Phys. Rev.* B **56** 4818–24
[46] Hayashi Sh, Tanimoto Sh and Yammamoto K 1990 *J. Appl. Phys.* **68** 5300–8
[47] DiMaria D, Dong D W, Falcony C, Theis T N, Kirtley J R, Tsang J C, Young D R, Pesavento F L and Brorson S D 1983 *J. Appl. Phys.* **54** 5801–27
[48] Nesheva D, Bineva I, Aneva Z and Hofmeister H 2005 *Thin Films and Coatings: New Research* ed B M Caruta (New York: Nova Science Publishers) pp 49–61